Sub-250 nm low-threshold deep-ultraviolet AlGaN-based heterostructure laser employing HfO_2/SiO_2 dielectric mirrors

Tsung-Ting Kao, Yuh-Shiuan Liu, Md. Mahbub Satter, Xiao-Hang Li, Zachary Lochner, P. Douglas Yoder, Theeradetch Detchprohm, Russell D. Dupuis' , Shyh-Chiang Shen' , Jae-Hyun Ryou' , Alec M. Fischer, Yong Wei, Hongen Xie, and Fernando A. Ponce

Citation: Appl. Phys. Lett. **103**, 211103 (2013); doi: 10.1063/1.4829477
View online: http://dx.doi.org/10.1063/1.4829477
View Table of Contents: http://aip.scitation.org/toc/apl/103/21
Published by the American Institute of Physics

Sub-250 nm low-threshold deep-ultraviolet AlGaN-based heterostructure laser employing HfO_2/SiO_2 dielectric mirrors

Tsung-Ting Kao,[1] Yuh-Shiuan Liu,[1] Md. Mahbub Satter,[1] Xiao-Hang Li,[1] Zachary Lochner,[1] P. Douglas Yoder,[1] Theeradetch Detchprohm,[1] Russell D. Dupuis,[1,a)] Shyh-Chiang Shen,[1,b)] Jae-Hyun Ryou,[1,c)] Alec M. Fischer,[2] Yong Wei,[2] Hongen Xie,[2] and Fernando A. Ponce[2]
[1]*School of Electrical and Computer Engineering, Georgia Institute of Technology, 777 Atlantic Dr. NW, Atlanta, Georgia 30332-0250, USA*
[2]*Department of Physics, Arizona State University, Tempe, Arizona 85287-1504, USA*

(Received 8 August 2013; accepted 25 October 2013; published online 18 November 2013)

We report a sub-250-nm, optically pumped, deep-ultraviolet laser using an $Al_xGa_{1-x}N$-based multi-quantum-well structure grown on a bulk Al-polar *c*-plane AlN substrate. TE-polarization-dominant lasing action was observed at room temperature with a threshold pumping power density of 250 kW/cm^2. After employing high-reflectivity SiO_2/HfO_2 dielectric mirrors on both facets, the threshold pumping power density was further reduced to 180 kW/cm^2. The internal loss and threshold modal gain can be calculated as 2 cm^{-1} and 10.9 cm^{-1}, respectively. © *2013 AIP Publishing LLC*. [http://dx.doi.org/10.1063/1.4829477]

III-nitride (III-N)-based optoelectronic devices have been actively studied and developed for over two decades. The wide range of the bandgap energy in III-N materials (from 0.7 eV to 6.2 eV) covers the full spectrum of photon emission from the near-infrared to deep-ultraviolet (DUV) wavelengths. Today, III-N-based solid state lighting is the viable technology for future energy-efficient light sources. High-quality DUV light emitting diodes (LEDs) have also been commercialized for water sanitation and bio-chemical agent detection applications. These UV emitters typically use an AlGaN alloy system to achieve wavelengths below 280 nm.[1–5] On the other hand, the development of DUV laser diodes (LDs) for $\lambda < 280$ nm has been challenging because of the challenges with achieving high free-carrier concentrations in both *p*-type and *n*-type AlGaN layers with high aluminum mole fraction and high defect densities, which arise from the lattice mismatch in epitaxial layers when these structures are grown on foreign substrates. As the photon emission wavelength decreases, the threshold power for laser action will also increase due to the fact that spontaneous emission rate increases and is approximately proportional to $1/\lambda^3$. To date, electrical carrier-injection LDs have not been reported for the lasing wavelength shorter than 336 nm.[6]

Recently, various AlGaN-based multiple-quantum-wells (MQWs) lasers with lasing wavelengths between 255 nm and 305 nm were reported under optical pumping conditions at room temperature (RT).[7–11] However, lasing actions in sub-250-nm region and internal laser parameters are rarely reported.[12,13] In our previous work, Lochner *et al.* demonstrated an optically pumped AlGaN-based MQW laser grown on an AlN substrate with an emission wavelength of ~243 nm and a threshold pumping power density (P_{th}) of 427 kW/cm^2.[13] To improve the lasing characteristics, dielectric mirrors coated on facets could be an effective approach to reduce the lasing threshold power. However, a proper choice of dielectric layers to achieve high-reflectivity end-mirrors for laser bars in the deep-UV (<250 nm) wavelengths has not yet been reported. In this paper, we report the lasing action from an AlGaN-based MQW laser with HfO_2/SiO_2 mirrors coated on both cleaved facets. Due to the large contrast of the refractive indices between HfO_2 ($n \sim 2.2$ and $k \sim 3 \times 10^{-3}$ cm^{-1} at $\lambda = 250$ nm) and SiO_2 ($n \sim 1.4$ and $k \sim 2.5 \times 10^{-3}$ cm^{-1} at $\lambda = 250$ nm),[14] distributed Bragg reflectors (DBRs) with high reflectivity ($R > 92\%$) and wide stop-band of ~60 nm were achieved by using a small number of HfO_2/SiO_2 pairs. The facet coatings effectively reduce the threshold pumping power density (P_{th}) of an AlGaN-based laser bar from 250 to 180 kW/cm^2 and lead to a reduction in threshold modal gain from 63 cm^{-1} to 10.9 cm^{-1}. The lasing peak is located at $\lambda = 249$ nm with a preferential transverse-electric (TE) polarization emission.

The AlGaN-based MQW structure was grown on an aluminum-polar (0001) native AlN substrate. Growth on a native substrate enables homoepitaxy of a buffer layer, which significantly reduces the density of dislocations in the epitaxial layers and improves subsequent active-region quality.[15] Prior to the growth, the AlN substrates were etched in a 3:1 H_2SO_4:H_2PO_4 acid solution at 90 °C for removing surface hydroxide.[16] The wafer was then annealed in a high-purity ammonia ambient at 1100 °C for the optimal condition for epitaxy. The epitaxial growth was performed in a Thomas-Swan (now Aixtron) 6 × 2 in. close-coupled showerhead metalorganic chemical vapor deposition (MOCVD) reactor system. Due to the low ad-atom mobility of Al atoms on the growing surface and parasitic gas-phase reaction between aluminum precursor and ammonia, high temperature, low pressure, and low V/III ratio are required for two-dimensional growth and smooth surface formation. In

[a)]Also at School of Materials Science and Engineering, Georgia Institute of Technology, 777 Atlantic Dr. NW, Atlanta, Georgia 30332-0250, USA.
[b)]Author to whom correspondence should be addressed. Electronic mail: shyh.shen@ece.gatech.edu
[c)]Current address: Department of Mechanical Engineering, University of Houston, Houston, Texas 77204-4006, USA.

this work, the relatively high growth temperature of 1130 °C at 75 Torr was used while the V/III ratios for AlN buffer layer and active region growth are set to less than 100 and approximately 400, respectively.

A cross-section of the layer structure is shown in Fig. 1(a). The active region consists of eight periods of quantum wells, with 3-nm $Al_{0.60}Ga_{0.40}N$ wells and 6-nm $Al_{0.75}Ga_{0.25}N$ barriers, between a 200-nm AlN buffer layer and an 8-nm AlN cap layer for surface passivation. In order to maximize the overlap between the optical field and the active region, any underlying AlGaN layers or superlattice structure for the purpose of strain reduction were omitted from the design. Fig. 1(b) shows the refractive index profile and the simulated optical field distribution within the laser structure. The refractive indices for ternary AlGaN alloys are calculated from the refractive indices of AlN and GaN using Vegard's law.[17] The optical confinement factor (Γ) is determined to be ~21.9% under the fundamental waveguide mode.

Fig. 2 shows the high-angle, asymmetric, (105)-reciprocal-space-mapping (RSM) of the epitaxial structure taken by a high-resolution triple-axis X-ray diffractometer. The vertical axis Q_y in the reciprocal lattice unit (rlu in $Å^{-1}$ unit) represents the reciprocal of the lattice constant *c* and the horizontal axis Q_x represents the reciprocal of the in-plane lattice constant *a*. The AlN peak and the AlGaN-based MQW peak (as guided by red-dashed curve) share the same Q_x value suggesting that the epitaxial grown layers are fully strained,

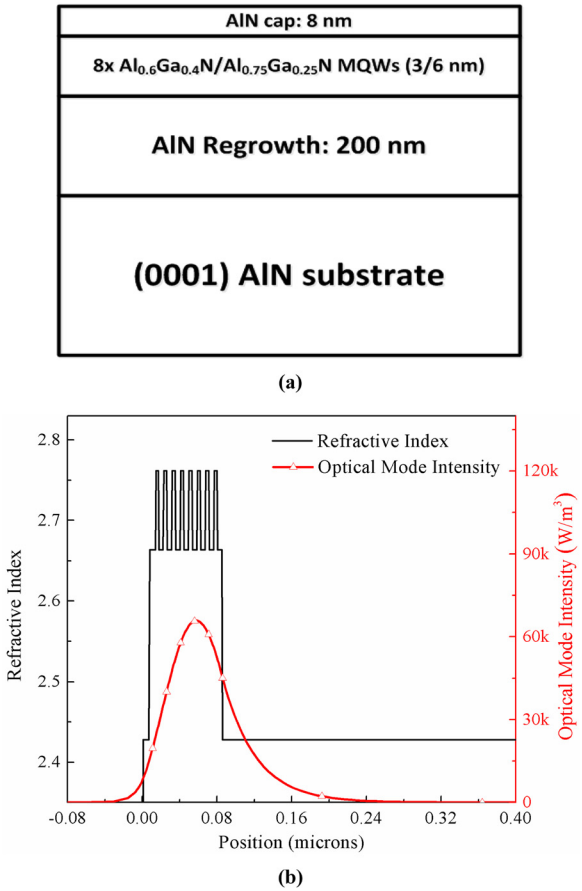

FIG. 1. (a) A schematic cross-sectional view of the AlGaN-based laser epitaxial structure. (b) The refractive index profile and simulated optical field distribution within the laser structure.

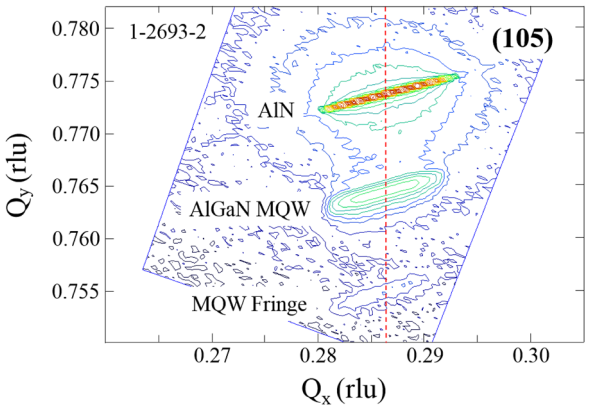

FIG. 2. RSM of the (105) AlGaN MQW and AlN diffraction peaks. The rlu represents the reciprocal lattice unit. The Q_x values of the peaks indicate the epitaxial layers are fully strained (i.e., pseudomorphically grown).

which inhibits the formation of defects such as cracks and dislocations associated with lattice relaxation. In addition, the first order fringe from the active region is clearly observed, suggesting smooth surface formation and high crystalline quality of the material.

Following the epitaxial growth, the wafer was thinned to 80 μm by a chemical-mechanical polishing process and Fabry-Perot Etalons were formed by cleaving along the *m*-plane of the sample into a 1.4-mm-long resonant cavity. Five and six pairs of HfO_2/SiO_2 DBR mirrors were sequentially deposited to form the front- and rear-side facet mirrors, respectively. The dielectric mirrors are tuned to a target of a center wavelength of 250 nm. Shown in Fig. 3(a) are the reflectivity spectra of the front-side and the backside facet mirrors deposited on the companion glass substrates using an ultraviolet-visible spectrometer (Shimadzu UV2401PC). Although the center wavelengths are slightly shifted due to processing variation, high-reflectivity mirrors with $R = 92\%$ and 97% at $\lambda = 249$ nm were achieved on the front- and rear-side facets, respectively.

The optical pumping experiment was performed by using an ArF excimer laser with an excitation wavelength of $\lambda = 193$ nm. The laser beam has a stripe width of 0.1 cm and stripe length of 1.3 cm. A detailed system setup is described elsewhere.[13] As shown in Fig. 3(a), the laser bar with double-sided dielectric mirror coatings has an emission peak at $\lambda = 249$ nm with a spectral line-width of 0.6 nm at maximum pumping power density of 265 kW/cm^2. The stimulated emission spectrum exhibits a preferential TE polarization, as shown in Fig. 3(b), with a degree of polarization (*P*), defined as $P = (I_{TE} - I_{TM})/(I_{TE} + I_{TM})$, approaching 100%. The TE-dominant emission is attributed to the in-plane compressive strain in the quantum-confined structure.[18] The optical output intensity measured before and after the facet coatings versus the excitation power density (*L-L* curve) is plotted in Fig. 4. The threshold pumping power density (P_{th}) was reduced by ~14%, from 250 to 215 kW/cm^2 after the first dielectric reflector ($R = 97\%$) was applied on the rear-side of the facet. Another 16% reduction in P_{th} (from 215 to 180 kW/cm^2) was also observed after the front-side high-reflectivity mirror ($R = 92\%$) was coated on the laser bar. We also observed a significant drop in the slope efficiency after both facet coatings were deposited, which suggests that

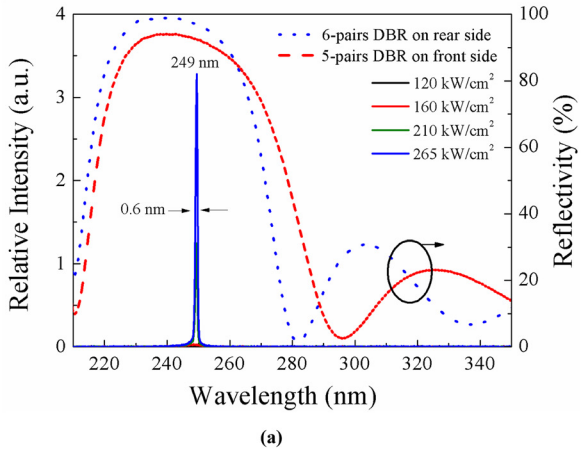

FIG. 3. (a) The power-dependent emission spectra of AlGaN-based MQW laser at RT with dielectric mirrors coated on both facets and the reflectivity spectra of 6-pairs and 5-pairs HfO_2/SiO_2 dielectric DBR mirrors. (b) The TE and TM-mode emission spectra of the same laser bar operating above the pump threshold at RT. An offset was applied on the TE emission spectrum for visual clarity.

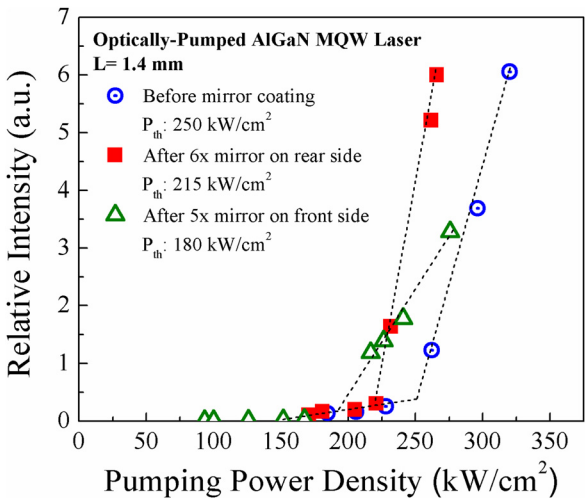

FIG. 4. Light-output intensity as a function of the optical pumping power density for the AlGaN-based MQW laser without the facet mirror coating (hollow circle in blue), after the rear-side mirror coating (solid square in red) and after the double-sided facet coating (hollow triangle in green).

a reduction in the cavity round-trip loss was achieved by the application of the DBRs on the cleaved facets.

The internal loss and the threshold gain of the AlGaN-based MQW laser can be estimated using the differences of the facet reflectivity before and after mirror coatings. Assuming the modal reflectance is close to the externally measured value from the companion glass substrates, the internal loss (α_i) can be determined through the following equation:[19]

$$\alpha_i = \frac{1}{L} \times \frac{\eta_d' - \eta_d}{\left(\frac{\eta_d}{\ln \frac{1}{\sqrt{R_1 R_2}}} - \frac{\eta_d'}{\ln \frac{1}{\sqrt{R_1' R_2'}}} \right)}, \tag{1}$$

where L ($=1.4$ mm) is the cavity length; R_1 and R_2 (both 18%) are the reflectivity of the as-cleaved facets; and R_1' (92%) and R_2' (97%) are the reflectivity of the front-side and the backside facets with the facet coatings, respectively. The differential quantum efficiency (η_d) of the cleaved laser bar can be obtained by

$$\eta_d \propto \frac{1}{F}\frac{dP_{out}}{dP_{in}} \propto \frac{1}{F}\frac{dI_{out}}{dP_{in}}, \tag{2}$$

where P_{in} and P_{out} represent the input and output power, respectively. The measured relative light output intensity is denoted as I_{out}; therefore, $\frac{dI_{out}}{dP_{in}}$ can be calculated from the L-L curves shown in Fig. 4. The differential quantum efficiency after the facet coating is denoted as η_d'. The fraction of the output power (F) measured from the front-side of the facet with respect to the total optical output power can be calculated by

$$F = \frac{1 - R_1}{(1 - R_1 + \sqrt{\frac{R_1}{R_2}}(1 - R_2)}. \tag{3}$$

In this case, F is 0.5 and 0.73 for the laser bar before and after facet coatings, respectively. Since the proportionality factors in the calculation of η_{d} and η_d' are identical. These parameters are canceled in Eq. (1), α_{i} can therefore be estimated to be $2\,\text{cm}^{-1}$. The threshold modal gain (g_{th}) can also be obtained by

$$\Gamma g_{th} = \alpha_i + \frac{1}{L}\ln\left(\frac{1}{\sqrt{R_1 R_2}}\right). \tag{4}$$

With the high-reflectivity facet mirrors coated on both sides of the laser bar, the g_{th} is reduced from $63\,\text{cm}^{-1}$ to $10.9\,\text{cm}^{-1}$. This reduction in the threshold modal gain shows the HfO_2/SiO_2 dielectric mirror can effectively enhance the performance of deep-UV lasers. It is also noted that g_{th} is approximately an order of magnitude lower than that of AlGaN-based MQWs grown on 6 H-SiC substrate at $\lambda \sim 250$ nm.[20]

In summary, we report an optically pumped, AlGaN-based, MQW laser with HfO_2/SiO_2 dielectric mirrors at room temperature. Employing high-reflectivity mirrors on the cleaved facets effectively reduces the threshold pumping power density of a deep-UV laser from 250 to 180 kW/cm^2. The lasing wavelength of 249 nm and a preferential TE-type

emission are observed with a degree of polarization ~100%. The internal loss and threshold gain of this deep-UV laser are estimated to be 2 cm^{-1} and 10.9 cm^{-1}, respectively.

This work was supported by the Defense Advanced Research Projects Agency under Contract No. FA2386-10-1-4152. R.D.D. acknowledges additional support of the Steve W. Chaddick Endowed Chair in Electro-Optics and the Georgia Research Alliance.

[1]J. R. Grandusky, S. R. Gibb, M. C. Mendrick, C. Moe, M. Wraback, and L. J. Schowalter, Appl. Phys. Express **4**, 082101 (2011).
[2]M. S. Shur and R. Gaska, IEEE Trans. Electron Devices **57**, 12 (2010).
[3]H. Hirayama, Y. Tsukada, T. Maeda, and N. Kamata, Appl. Phys. Express **3**, 031002 (2010).
[4]V. Adivarahan, A. Heidari, B. Zhang, Q. Fareed, S. Hwang, M. Islam, and A. Khan, Appl. Phys. Express **2**, 102101 (2009).
[5]A. Yasan, R. McClintock, K. Myes, D. Shiell, L. Gautero, S. Darvish, P. Kung, and M. Razeghi, Appl. Phys. Lett. **83**, 4701 (2003).
[6]H. Yoshida, Y. Yamashita, M. Kuwabara, and H. Kan, Appl. Phys. Lett. **93**, 241106 (2008).
[7]J. Xie, S. Mita, Z. Bryan, W. Guo, L. Hussey, B. Moody, R. Schlesser, R. Kirste, M. Gerhold, R. Collazo, and Z. Sitar, Appl. Phys. Lett. **102**, 171102 (2013).
[8]V. N. Jmerik, A. M. Mizerov, A. A. Sitnikova, P. S. Kop'ev, S. V. Ivanov, E. V. Lutsenko, N. P. Tarasuk, N. V. Rzheutskii, and G. P. Yablonskii, Appl. Phys. Lett. **96**, 141112 (2010).
[9]T. Wunderer, C. L. Chua, Z. Yang, J. E. Northrup, N. M. Johnson, G. A. Garrett, H. Shen, and M. Wraback, Appl. Phys. Express **4**, 092101 (2011).
[10]J. Mickevičius, J. Jurkevičius, K. Kazlauskas, A. Žukauskas, G. Tamulaitis, M. S. Shur, M. Shatalov, J. Yang, and R. Gaska, Appl. Phys. Lett. **100**, 081902 (2012).
[11]Z. Lochner, X. H. Li, T. T. Kao, Md. M. Satter, H. J. Kim, S. C. Shen, P. D. Yoder, J. H. Ryou, R. D. Dupuis, K. Sun, Y. W, T. Li, A. Fischer, and F. A. Ponce, Phys. Status Solidi (A) **210**, 1768–1770 (2013).
[12]T. Takano, Y. Narita, A. Horiuchi, and H. Kawanishi, Appl. Phys. Lett. **84**, 3567 (2004).
[13]Z. Lochner, T. T. Kao, Y. S. Liu, X. H. Li, Md. M. Satter, S. C. Shen, P. D. Yoder, J. H. Ryou, R. D. Dupuis, Y. O. Wei, H. Xie, A. Fischer, and F. A. Ponce, Appl. Phys. Lett. **102**, 101110 (2013).
[14]P. Torchio, A. Gatto, M. Alvisi, G. Albrand, N. Kaiser, and C. Amra, Appl. Opt. **41**, 3256 (2002).
[15]M. Kneissl, Z. Yang, M. Teepe, C. Knollenberg, O. Schmidt, P. Kiesel, N. M. Johnson, S. Schujiman, and L. J. Schowalter, J. Appl. Phys. **101**, 123103 (2007).
[16]A. Rice, R. Collazo, J. Tweedie, R. Dalmau, S. Mita, J. Xie, and Z. Sitar, J. Appl. Phys. **108**, 043510 (2010).
[17]M. E. Levinshtein, S. L. Rumyantsev, and M. S. Shur, *Properties of Advanced Semiconductor Materials GaN, AlN, InN, BN, SiC, SiGe* (Wiley, New York, 2001).
[18]R. G. Banal, M. Funato, and Y. Kawakami, Phys. Rev. B **79**, 121308 (2009).
[19]L. A. Coldren and S. W. Corzine, *Diode Lasers and Photonic Integrated Circuits*, 1st ed. (Wiley, New York, 1995).
[20]E. F. Pecora, W. Zhang, A. Y. Nikiforov, J. Yin, R. Paiella, L. D. Negro, and T. D. Moustakas, J. Appl. Phys. **113**, 013106 (2013).